Comparison between Iron and Ruthenium Reagents Mediating Gif IV Type Oxygenation of Cyclohexane §

ARTICLE *in* INORGANIC CHEMISTRY · OCTOBER 2000

Impact Factor: 4.76 · DOI: 10.1021/ic0001560

5 AUTHORS, INCLUDING:

David T. Richens
The University of Waikato
105 PUBLICATIONS **1,698** CITATIONS

Comparison between Iron and Ruthenium Reagents Mediating Gif^{IV}-Type Oxygenation of Cyclohexane[§]

Scott B. Marr,[†] Richard O. Carvel,[†] David T. Richens,*[,†] Hyun-Jin Lee,[‡] Michael Lane,[‡] and Pericles Stavropoulos*[,‡]

School of Chemistry, University of St. Andrews, North Haugh, St. Andrews, KY16 9ST, Scotland, U.K., and the Department of Chemistry, Boston University, Boston, Massachusetts 02215

Received February 14, 2000

A ruthenium-based version of Barton's Gif^{IV}-type system ($Ru_{cat}/Zn/O_2$ in pyridine/acetic acid) for the selective oxygenation of cycloalkanes has been studied in detail for the first time using a range of analytical techniques. The system, based on the use of the triruthenium complex $[Ru_3O(O_2CCH_3)_6(py)_3]$ in the presence of zinc powder in aerated pyridine/acetic acid (10:1 v/v), affords yields of cyclohexanone (main product) and cyclohexanol from cyclohexane comparable to that of the well-studied iron system based on the use of $[Fe_3O(O_2CCH_3)_6(py)_3]\cdot py$ but with a lower selectivity for the ketone product. The time taken for the appearance and distribution of the -one/-ol products is different for the two metals and also depends on the efficiency of stirring of the zinc powder. The differing -one/-ol ratios and their times of appearance have been correlated with competing reactions on the intermediate cyclohexylhydroperoxide, most likely generated via oxygen- and carbon-centered radical chemistry. The appearance of cyclohexanol much earlier in the reaction for the ruthenium-based system has been traced to a slower assembly reaction for ruthenium to form the species responsible for the ketonization step, which allows production of alcohol via zinc reduction of cyclohexylhydroperoxide to compete successfully. Extensive investigations into the nature of the metal species present during turnover, using cyclic voltammetry, ^{1}H NMR, and UV−vis spectroscopy, show that for either system the divalent monomeric complex *trans*-$[M(O_2CCH_3)_2(py)_4]$ (M = Ru or Fe) is the major species present during the appearance of ketone product. Use of *trans*-$[Fe(O_2CCH_3)_2(py)_4]$ as the precursor reagent results in the highest Gif^{IV} activity (conversion yield) toward cyclohexane oxygenation. It is concluded that formation of *sec*-alkylhydroperoxides in addition to monomeric divalent complexes such as *trans*-$[M(O_2CCH_3)_2(py)_4]$ (M = Fe or Ru) are key processes central to the mechanism of the Gif oxygenation process toward ring hydrocarbons. The combination Fe(II)/ROOH is considered responsible for the formation of ketone (and some alcohol), most likely via Haber−Weiss chemistry, in competition with formation of alcohol via Zn reduction of ROOH.

Introduction

Considerable interest continues to surround the search for active and selective metal complex catalysts for the oxygenation of unactivated hydrocarbon substrates via O_2 under ambient conditions.[1,2] The Gif catalytic systems, developed by Barton and co-workers over the past 15 years, have proved to be among the most active and moreover selective catalytic systems under ambient conditions for the monoxygenation of cycloalkanes to give ketone products.[3−5] Few systems can match the high turnover numbers (>1000 in less than 1 day) as well as the unusually high selectivity to the ketone, as shown by both the early iron-based Gif^{IV}-type systems ($Fe_{cat}/Zn/O_2$) and the more recent H_2O_2-dependent analogues ("GoAgg" versions), the latter relying on combinations of simple iron salts such as $FeCl_3$ and H_2O_2.[4] For maximum activity and efficiency these systems work most effectively in pyridine/acetic acid, although addition of picolinic acid to solutions of $FeCl_3$ has been shown[6] to increase the rate of the catalytic reaction by 50-fold.

In Gif^{IV}-type oxygenation systems the trinuclear complex $[Fe_3O(O_2CCH_3)_6(py)_3]\cdot py$ (**1**) has been frequently used as the added iron reagent[3b] in conjunction with zinc powder (reductant) in aerated pyridine/acetic acid (10:1 v/v). This system remains

§ Submitted in the memory of Sir Derek H. R. Barton.

† University of St. Andrews.

‡ Boston University.

(1) (a) Sheldon, R. A. *New Developments in Selective Oxidation*; Academic Press: Amsterdam, 1990. (b) Sheldon, R. A. *J. Chem. Technol. Biotechnol.* **1997**, *68*, 381. (c) *Activation and Functionalization of Alkanes*; Hill, C. L., Ed.; John Wiley & Sons: New York, 1989. (d) *Metal Catalyzed Oxidations of Organic Compounds*; Sheldon, R. A., Kochi, J. K., Eds.; Academic Press: New York, 1981; p. 340. (e) Mimoun, M. In *Comprehensive Coordination Chemistry*; Wilkinson, G., Gillard, R. D., McCleverty, J. A., Eds.; Pergamon Press: Oxford, 1987; Vol. 6, pp 317−410.

(2) (a) Goldstein, A. S.; Drago, R. S. *Inorg. Chem.* **1991**, *30*, 4506 and references therein. (b) Maldotti, A.; Bartocci, C.; Amadelli, R.; Polo, E.; Battioni, P.; Mansuy, D. *J. Chem. Soc., Chem. Commun.* **1991**, 1487.

(3) (a) Barton, D. H. R. *Chem. Soc. Revs.* **1996**, *25*, 237 and references therein. (b) Barton, D. H. R.; Doller, D. *Acc. Chem. Res.* **1992**, *25*, 504. (c) Barton, D. H. R. *Aldrichim. Acta* **1990**, *23*, 3. (d) Barton, D. H. R.; Boivin, J.; Gastiger, M.; Morzychi, J.; Hay-Motherwell, R. S.; Motherwell, W. B.; Ozbalik, N.; Schwartzentruber, K. M. *J. Chem. Soc., Perkin Trans. 1* **1986**, 947. (e) Barton, D. H. R.; Boivin, J.; Lelandais, P. *J. Chem. Soc., Perkin Trans. 1* **1989**, 463. (f) Balavoine, G.; Barton, D. H. R.; Boivin, J.; LeCoupanec, P.; Lelandais, P. *New J. Chem.* **1989**, *13*, 691.

(4) Barton, D. H. R.; Malley, F.; Ozbalik, N.; Schmitt, M.; Young, E.; Balavoine, G. *J. Am. Chem. Soc.* **1989**, *111*, 7144.

(5) (a) Barton, D. H. R.; Hu, B.; Taylor, D. K.; Rojas-Wahl, R. U. *J. Chem. Soc., Perkin Trans. 2* **1996**, 1031. (b) Sawyer, D. T.; Sobkowiak, A.; Matsushita, T. *Acc. Chem. Res.* **1996**, *29*, 409 and references therein.

(6) (a) Balavoine, G.; Barton, D. H. R.; Boivin, J.; Gref, A. *Tetrahedron Lett.* **1990**, *3*, 659. (b) Tung, H.-C.; Kang, C.; Sawyer, D. T. *J. Am. Chem. Soc.* **1992**, *114*, 3445.

10.1021/ic0001560 CCC: $19.00
Published on Web 09/13/2000

of considerable interest owing to the desirable use of molecular dioxygen as the primary oxygen source and the potential biomimetic analogies. Despite significant advances in the elucidation of structural and mechanistic elements involved in these reactions, very little is specifically known about the nature of the metal species present during active turnover[5] and whether the observed product profile (high ketone selectivity) can be traced to favorable generation of and subsequent reactions involving the secondary alkylhydroperoxide, which has been detected as an intermediate in $FeCl_3/H_2O_2$ mediated oxygenation of cyclohexane.[7]

In relation to cyclohexylhydroperoxide, two diametrically opposing hypotheses have been advanced to interpret the mode of its formation. The original Barton mechanism[3] (eqs 1−4),

$$Fe^{III} + H_2O_2 \rightarrow Fe^{V}{=}O + H_2O \quad (1)$$

$$Fe^{V}{=}O + c\text{-}C_6H_{12} \rightarrow Fe^{V}(OH)(c\text{-}C_6H_{11}) \quad (2)$$

$$Fe^{V}(OH)(c\text{-}C_6H_{11}) + H_2O_2 \rightarrow Fe^{III}(OH)(c\text{-}C_6H_{11}) + O_2 + 2H^+ \quad (3)$$

$$Fe^{III}(OH)(c\text{-}C_6H_{11}) + O_2 \rightarrow Fe^{III}(OH)(OO\text{-}c\text{-}C_6H_{11}) + H_2O \leftrightarrow Fe^{III} + 2OH^- + c\text{-}C_6H_{11}OOH \quad (4)$$

invokes a nonradical [2 + 2] C−H activation by high-valent $Fe^{V}{=}O$ units to generate metal−cyclohexyl intermediates, which eventually undergo dioxygen insertion to form *metal-bound* cyclohexylperoxyl species.

In contrast, investigations by Minisci[8] and Ingold[9] on *t*-BuOOH-dependent Gif reagents, and the related "oxygenated Fenton" systems,[5b] have provided compelling evidence in support of a radical mechanism via formation of a *diffusively free* substrate centered alkyl and alkylperoxyl radicals (eqs 5−9):

$$Fe^{II} + t\text{-}BuOOH \rightarrow Fe^{III} + OH^- + t\text{-}BuO^{\bullet} \quad (5)$$

$$Fe^{III} + t\text{-}BuOOH \rightarrow Fe^{II} + H^+ + t\text{-}BuOO^{\bullet} \quad (6)$$

$$t\text{-}BuO^{\bullet} + c\text{-}C_6H_{12} \rightarrow t\text{-}BuOH + c\text{-}C_6H_{11}^{\bullet} \quad (7)$$

$$c\text{-}C_6H_{11}^{\bullet} + O_2 \rightarrow c\text{-}C_6H_{11}OO^{\bullet} \quad (8)$$

$$c\text{-}C_6H_{11}OO^{\bullet} + t\text{-}BuOOH \rightarrow c\text{-}C_6H_{11}OOH + t\text{-}BuOO^{\bullet} \quad (9)$$

There is now consensus[10] that these systems operate because of the action of *t*-BuO$^{\bullet}$/*t*-BuOO$^{\bullet}$ radicals. Recently this Haber−Weiss−Walling mechanism[11] has been conceptually[12] and experimentally[13] validated for Gif reagents centered on $Fe^{II/III}/H_2O_2$ combinations.

In the present investigation we compare the activity of **1** with

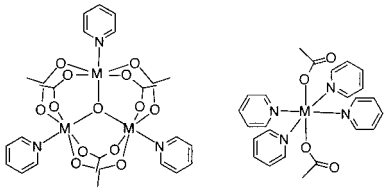

1 M = Fe
2 M = Ru

3 M = Fe
4 M = Ru

its triruthenium analogue $[Ru_3O(O_2CCH_3)_6(py)_3]$ (**2**) toward Gif^{IV} oxygenations on cyclohexane under similar conditions. Both generate highly active Gif^{IV} catalysts, a feature that has been correlated with the rapid formation in these solutions of divalent monomeric complexes, principally *trans*-$[M(O_2CCH_3)_2(py)_4]$ (M = Fe (**3**) or Ru (**4**)). The rates of formation of and subsequent reactions involving the two respective monomeric complexes are believed to be directly linked to the different product profiles (ketone versus *sec*-alcohol) seen in comparative Gif^{IV} studies carried out previously in our laboratories.[14]

Experimental Section

Preparation of Compounds. Unless otherwise noted, all operations involving synthesis of iron and ruthenium complexes were performed under a pure dinitrogen or argon atmosphere, using Schlenk techniques on an inert gas/vacuum manifold or in a drybox (O_2, H_2O < 1 ppm). Hexane, petroleum ether, and toluene were distilled over Na, and THF and diethyl ether were distilled over Na/Ph_2CO. Acetonitrile and methylene chloride were distilled over CaH_2. Ethanol and methanol were distilled over the corresponding magnesium alkoxide, and acetone was distilled over drierite. Pyridine was distilled over calcium hydride onto freshly dried 4 Å molecular sieves. Doubly distilled acetic acid (metallic impurities in parts per trillion) was purchased from Aldrich. Cyclohexane was purified by washing with concentrated sulfuric acid followed by water, 5% sodium hydroxide solution, and water again until neutral. After drying over anhydrous magnesium sulfate, it was distilled over calcium hydride onto freshly dried 4 Å molecular sieves. Deuterated solvents for NMR experiments were purchased from Cambridge Isotope Laboratory, with the exception of pyridine-d_5 (99.5% D) (Fluorochem) and acetic acid-d_4 (99.9% D) (Aldrich), which were used as supplied for the ^{1}H NMR experiments. Zinc powder was used as supplied or preconditioned by treatment with aqueous 2 M HCl, washed with water and pyridine, and dried under vacuum (10^{-2} Torr) for 4 h. Samples of $[Fe_3^{II,III,III}O(O_2CCH_3)_6(py)_3]\cdot py$ (**1**),[15] $[Ru_3^{II,III,III}(O_2CCH_3)_6(py)_3]$ (**2**),[16] *trans*-$[Fe^{II}(O_2CCH_3)_2(py)_4]$ (**3**),[17] and $[Ru^{III}{}_3(O_2CCH_3)_6(py)_3](PF_6)$[18] were prepared according to published synthetic methods. Samples of *trans*-$[Ru^{II}(O_2CCH_3)_2(py)_4]$ (**4**) have been prepared

(7) (a) Barton, D. H. R.; Bévière, S. D.; Chavasiri, W.; Csuhai, E.; Doller, D.; Liu, W. G. *J. Am. Chem. Soc*. **1992**, *114*, 2147. (b) Barton, D. H. R.; Csuhai, E.; Doller, D.; Balavoine, G. *J. Chem. Soc., Chem. Commun*. **1990**, 1787.

(8) (a) Minisci, F.; Fontana, F.; Araneo, S.; Recupero, F.; Zhao, L. *Synlett* **1996**, 119. (b) Minisci, F.; Fontana, F.; Araneo, S.; Recupero, F.; Banfi, S.; Quici, S. *J. Am. Chem. Soc*. **1995**, *117*, 226. (c) Minisci, F.; Fontana, F.; Araneo, S.; Recupero, F. *J. Chem. Soc., Chem. Commun*. **1994**, 1823. (d) Minisci, F.; Fontana, F. *Tetrahedron Lett*. **1994**, *35*, 1427.

(9) (a) Snelgrove, D. W.; MacFaul, P. A.; Ingold, K. U.; Wayner, D. D. M. *Tetrahedron Lett*. **1996**, *37*, 823. (b) MacFaul, P. A.; Wayner, D. D. M.; Ingold, K. U. *Acc. Chem. Res*. **1998**, *31*, 159.

(10) (a) Barton, D. H. R. *Synlett* **1997**, 229. (b) Barton, D. H. R.; Le Gloahec, V. N.; Patin, H.; Launay, F. *New J. Chem*. **1998**, *22*, 559. (c) Barton, D. H. R.; Le Gloahec, V. N.; Patin, H. *New J. Chem*. **1998**, *22*, 565.

(11) (a) Walling, C. *Acc. Chem. Res*. **1998**, *31*, 155. (b) Walling, C. *Chem. Res*. **1975**, *8*, 125.

(12) Perkins, M. J. *Chem. Soc. Rev*. **1996**, 229.

(13) (a) Newcomb, M.; Simakov, P. A.; Park, S.-U. *Tetrahedron Lett*. **1996**, *37*, 819. (b) Knight, C.; Perkins, M. J. *J. Chem. Soc., Chem. Commun*. **1991**, 925. (c) Kiani, S.; Tapper, A.; Staples, R. J.; Stavropoulos, P. *J. Am. Chem. Soc*. **2000**, *122*, 7503. (d) Tapper, A.; Long, J. R.; Staples, R. J.; Stavropoulos, P. *Angew. Chem., Int. Ed. Engl*. **2000**, *39*, 2343.

(14) Powell, G.; Richens, D. T.; Khan, L. *J. Chem. Res*. **1994**, 507.

(15) Sorai, M.; Kaji, K.; Hendrickson, D. N.; Oh, S. M. *J. Am. Chem. Soc*. **1986**, *108*, 702.

(16) (a) Dziobkowski, C. T.; Wrobleski, J. T.; Brown, D. B. *Inorg. Chem*. **1981**, *20*, 671, 679. (b) Spencer, A.; Wilkinson, G. *J. Chem. Soc., Dalton Trans*. **1972**, 1570.

(17) (a) Singh, B.; Long, J. R.; Fabrizi de Biani, F.; Gatteschi, D.; Stavropoulos, P. *J. Am. Chem. Soc*. **1997**, *119*, 7030. (b) Singh, B.; Long, J. R.; Papaefthymiou, G. C.; Stavropoulos, P. *J. Am. Chem. Soc*. **1996**, *118*, 5824.

(18) Baumann, J. A.; Salmon, D. J.; Wilson, S. T.; Meyer, T. J.; Hatfield, W. E. *Inorg. Chem*. **1978**, *17*, 3342.

previously following treatment of methanolic solutions of $[Ru^{II}_2(O_2CCH_3)_4]$ with pyridine.[19] However, $[Ru^{II}_2(O_2CCH_3)_4]$ is not synthesized in a straightforward manner and the preparation of **4** described here via treatment of **2** with zinc powder in pyridine/acetic acid offers a more facile route relevant to the catalytic pathway. All other chemicals were purchased from Aldrich (highest available purities) and used as supplied without further purification.

$[Ru^{II}(O_2CCH_3)_2(py)_4]$ (4) via Zinc Reduction of 2. Yellow-brown crystals of $[Ru_3^{II,III,III}(O_2CCH_3)_6(py)_3]$ (**2**) (200 mg, 0.22 mmol) or blue powder of $[Ru^{III}_3(O_2CCH_3)_6(py)_3](PF_6)$ (232 mg, 0.22 mmol) are dissolved in a mixture of pyridine (20.0 mL) and acetic acid (2.0 mL). Zinc powder (1.32 g, 20 mmol) is added to this solution, and the mixture is stirred vigorously for 1 h. The resulting orange-red mixture is filtered twice to remove the remaining Zn dust, and the filtrate is reduced under vacuum to 5 mL. Slow diffusion of diethyl ether into the clear orange-red solution at −20 °C affords orange crystals of $[Ru^{II}(O_2CCH_3)_2(py)_4]$ (**4**) (240 mg, 0.45 mmol, 68%). ^{1}H NMR (benzene-d_6): δ 8.798 (dd, 4H, 2*H*-py), 6.864 (t, 2H, 4*H*-py), 6.571 (t, 4H, 3*H*-py), 2.244 (s, 3H, O_2CCH_3). Anal. Calcd for $C_{24}H_{26}N_4O_4Ru_1$: C, 53.82; H, 4.89; N, 10.46. Found: C, 53.68; H, 4.94; N, 10.36.

General Procedure for Gif^{IV}-Type Oxygenations. The Gif^{IV}-type oxygenations of cyclohexane were carried out in 100 mL round-bottomed flasks (B24 ground glass) and stirred with a 2 cm long "rugby-ball-shaped" magnetic follower. The catalyst (14 μmol), cyclohexane (2.15 mL, 20 mmol), and glacial acetic acid (4.6 mL, 80 mmol) were stirred at a constant predefined stirring rate (750 or 1000 rpm) in a solution of pyridine (56 mL) at 20 °C. The reaction was initiated by the addition of zinc powder (2.6 g, 39.7 mmol), which was prepared for use by gentle grinding to remove any lumps. During the entire reaction period the reaction flask was open to the atmosphere via the B24 ground glass socket.

A small aliquot of the reaction solution (2.0 mL) was removed after a set time interval and quenched by the careful addition of 5 mL of 20% aqueous sulfuric acid. The organic components were extracted with three 5 mL portions of diethyl ether, and the combined ethereal extract was then washed with a saturated sodium bicarbonate solution (5 mL) and then dried over anhydrous magnesium sulfate. During this whole procedure stoppers were kept on the flasks to minimize evaporation of the ethereal extract. A portion of the dried extract (2 mL) was then accurately measured out with a pipet, and cyclooctane (1.5 μL) was added as an internal standard for analysis.

Product Quantification by GC−MS. Analysis of the extracts (1 μL volume) was carried out in triplicate by quantitative GC−MS on a Hewlett-Packard gas chromatograph (GC) coupled to a Finnegan Matt INCOS 50 mass spectrometer. The GC was fitted with a SGE BP1 capillary column (25 m, 0.22 mm i.d., film thickness of 0.10 μm, stationary phase of 100% dimethyl polysiloxane). Helium was utilized as the carrier gas. The following temperature program was used: initial temperature 40 °C, final temperature 150 °C, rate of temperature increase 20 °C min^{-1}. This program was necessary to achieve a good separation of pyridine from the products and the cyclooctane internal standard. It was not, however, possible using the available capillary column to separate cyclohexanone (-one) from cyclohexanol (-ol). Therefore, a method was devised for their individual analysis based on using standard mixtures of -one and -ol, wherein integrated ion masses specific to each were first obtained (GC−MS), and these were then summed. This method was possible because the two compounds possessed a number of intense MS peaks specific to each and allowed for satisfactory integration and good reproducibility, as documented with known -one/-ol mixtures for which excellent results (±5%) were obtained. Because of fluctuations in the output signal from the GC−MS, it proved necessary to construct a fresh calibration curve each day, using a total of 15 separate injections from five standard solutions of -one and -ol (2 mL samples containing cyclooctane (1.5 μL) as internal standard). The ether extraction efficiency was also tested on standard solutions of -one and -ol in pyridine/acetic acid (10:1 v/v) with no catalyst present, using the same quenching method and quantitative GC−MS analysis, and was >98% satisfactory in all cases.

Electrochemistry. Cyclic voltammetric experiments were carried out on 5 mmol dm^{-3} solutions of the metal species in distilled reagent-grade pyridine (Fisons) or 10:1 pyridine/acetic acid solutions (10:1 v/v) as required (0.1 M $[Bu_4N](PF_6)$ electrolyte), using a standard three-electrode cell comprising a glassy-carbon disk working electrode (area, 0.1 cm^2), a Pt-wire counter electrode, and a Ag/AgCl reference electrode. Deoxygenation was carried out with a stream of argon gas. The potential of the working electrode was controlled using a Princeton Applied Research model 170 electrochemistry system with a built-in ramp generator and an *XY* plotter or controlled using a PINE Instrument RDE4 potentiostat with a Graphtec WX3000 *XY* recorder. The potential was monitored with a Fluke model 8010A high-impediance digital voltmeter. An *iR* compensation of approximately 100 mV was applied across the working and reference electrodes. Typical scan rates were 0.1 V s^{-1}. All potentials are reported relative to the Ag/AgCl electrode at 25 °C. $[Bu_4N](PF_6)$ was recrystallized from ethanol and dried in a vacuum oven at 100 °C prior to use.

^{1}H NMR Monitoring of Catalytic Reaction Mixtures. (a) Iron-Based Gif^{IV}-Type Reaction. $[Fe_3O(O_2CCH_3)_6(py)_3]\cdot$py (**1**) (2.0 mg, 2.46 μmol) was dissolved in a mixture of pyridine-d_5 (10.0 mL, 99.5% D) and acetic acid-d_4 (1.0 mL, 99.9% D) to which cyclohexane (0.12 mL) and zinc powder (430 mg, 6.57 mmol) were added. These were stirred efficiently with the aid of a small (10 mm) magnetic follower in a 25 mL B14 round-bottomed flask fitted with a $CaCl_2$ drying tube. At intervals of 0.5, 1, 1.5, 2, 3, 4, 5, 5.5, and 12.5 h, samples (0.5 mL) of the reaction were removed and ^{1}H NMR spectra recorded in the range δ −2 to 11 ppm versus TMS.

(b) Ruthenium Based Gif^{IV}-Type Reaction. $[Ru_3O(O_2CCH_3)_6(py)_3]$ (**2**) (1.2 mg, 1.32 μmol) was dissolved in a mixture of pyridine-d_5 (5 mL, 99.5% D) and acetic acid-d_4 (0.5 mL, 99.9% D) to which cyclohexane (0.1 mL) and zinc powder (230 mg, 3.52 mmol) were combined in a 10 mL B14 round-bottomed flask fitted with a $CaCl_2$ drying tube. The mixture was stirred efficiently in the open atmosphere with the aid of a small (10 mm) magnetic follower. Reaction aliquots were removed and ^{1}H NMR spectra recorded as described for the iron reaction above.

(c) Fate of the Ru Species under Gif^{IV}-Type Conditions. A sample of $[Ru_3O(O_2CCH_3)_6(py)_3]$ (**2**) (62 mg, 68 μmol) was dissolved in a mixture of pyridine-d_5 (5 mL, 99.5% D) and acetic acid-d_4 (0.5 mL, 99.9% D). Zinc powder (218 mg, 3.34 mmol) was added, and the mixture was stirred well in a 10 mL B14 round-bottomed flask fitted with a $CaCl_2$ drying tube. Samples (0.5 mL) were removed at various time intervals, the zinc was filtered off, and ^{1}H NMR spectra were recorded in standard 5 mm tubes. For runs carried out in neat pyridine-d_5 the zinc was preconditioned as described above.

X-ray Structure Determination. Crystallographic data for $[Ru_3O(O_2CCH_3)_6(py)_3]$ (**2**) are provided as Supporting Information in CIF format. Crystallographic data are presented in Table 1. Hexagonally shaped, yellow-brown single crystals of **2** were picked from the crystallization vessel, coated with Paratone-N oil because of air sensitivity and/or desolvation, mounted on a glass fiber using grease, and transferred to a Siemens (Bruker) SMART CCD (charge-coupled device) based diffractometer equipped with an LT-2 low-temperature apparatus operating at 213 K. Data were measured using ω scans of 0.3° per frame for 30 s such that a hemisphere was collected. A total of 1271 frames were collected with a maximum resolution of 0.75 Å. The first 50 frames were re-collected at the end of data collection to monitor for decay. Cell parameters were retrieved using SMART software[20] and refined using the SAINT software,[21] which corrects for Lp and decay. Absorption corrections were applied using SADABS[22] supplied by George Sheldrick. The structure is solved by the direct

(19) (a) Lindsay, A. J.; Wilkinson, G.; Motevalli, M.; Hursthouse, M. B. *J. Chem. Soc., Dalton Trans.* **1987**, 2723. (b) Stephenson, T. A.; Wilkinson, G. *J. Inorg. Nucl. Chem.* **1966**, *28*, 2285.

(20) *SMART, Software for the CCD Detector System*, version 5.050 (NT); Bruker Analytical X-ray Systems: Madison, WI, 1998.

(21) *SAINT, Software for the CCD Detector System*, version 5.01 (NT); Bruker Analytical X-ray Systems: Madison, WI, 1998.

(22) Blessing, R. H. SADABS, Program for Absorption Corrections Using Siemens CCD Based on the Method of Robert Blessing. *Acta Crystallogr*. **1995**, *A51*, 33−38.

method using the SHELXS-97[23] program and refined by the least-squares method on F^2, SHELXL-97,[24] incorporated in SHELXTL-PC, version 5.10.[25]

The structure was solved in the space group *R*3 (No. 146) by analysis of systematic absences. All non-hydrogen atoms are refined anisotropically. Hydrogens were calculated by geometrical methods and refined as a riding model. The crystal used for the diffraction studies showed no decomposition during data collection. The drawing (Supporting Information) is done at 50% probability ellipsoids.

Other Physical Measurements. ^{1}H NMR spectra were recorded in standard 5 mm tubes on a Bruker AM-300 instrument or a Varian XL-400 NMR spectrometer operating at 300 or 400 MHz, respectively. Chemical shifts were reported relative to tetramethylsilane (TMS) as the internal reference. FT-IR spectra were obtained on a Perkin-Elmer 1800 spectrometer. UV−vis spectra were obtained on a Perkin-Elmer Lambda 14P scanning spectrophotometer using 1 cm quartz cuvettes or on a Hewlett-Packard 8452A diode array spectrometer. Metal compounds were routinely checked for purity by elemental analysis on a CHN Carlo Erba 1106 instrument. Microanalysis for compounds **4** was done by H. Kolbe, Mikroanalytisches Laboratorium, Mülheim an der Ruhr, Germany.

Results and Discussion

Synthesis and Characterization of Compounds. The iron compounds used in the present study have been previously described.[17] In this section, we concentrate on the preparation of the corresponding ruthenium species from stoichiometric reactions, under conditions relevant to catalysis.

Different preparation protocols for $[Ru_3O(O_2CCH_3)_6(py)_3]$ (**2**) have been described in the literature.[16,18] We find that one-electron reduction of a blue solution of $[Ru^{III}_3O(O_2CCH_3)_6(py)_3](PF_6)$ in CH_3OH by hydrazine hydrate ($NH_2NH_2\cdot H_2O$) provides most reliably a greenish powder of **2**, which after the prescribed washings is of sufficient purity for further studies.[18] Analytically pure material is obtained by recrystallization upon diffusion of diethyl ether into a solution of crude **2** in py/AcOH (10:1 v/v). The so-obtained yellow-brown crystals of **2** are confirmed by single-crystal X-ray analysis to feature the expected trinuclear oxo-bridged core (Supporting Information), which by virtue of the crystallographically imposed D_3 symmetry does not distinguish between sites of different oxidation states. In contrast to $[Fe_3O(O_2CCH_3)_6(py)_3]\cdot$py (**1**), no solvated pyridine is observed in the structure of **2**. Moreover, unlike **1**, compound **2** is known to be air-sensitive, especially in solutions, slowly affording the blue cation $[Ru^{III}_3O(O_2CCH_3)_6(py)_3]^+$ ($[\mathbf{2}]^+$). Thus, greenish samples of **2** are frequently contaminated with the one-electron-oxidized $[\mathbf{2}]^+$. As first disclosed by Meyer and co-workers,[26] ^{1}H NMR spectra of mixtures of **2**/$[\mathbf{2}]^+$ still feature only one set of pyridine- and acetate-derived resonances, albeit shifted to values between those observed for the pure materials, due to rapid charge transfer between **2** and $[\mathbf{2}]^+$ on the NMR time scale.

Reduction of **2** by Zn powder in py/AcOH (10:1 v/v) for 1 h or more affords orange-red solutions from which orange crystals of *trans*-$[Ru^{II}(O_2CCH_3)_2(py)_4]$ (**4**) are readily obtained upon diffusion of diethyl ether. Microanalytical and ^{1}H NMR data confirm this assignment, as does a low-resolution X-ray analysis on a poor-quality crystal of **4**. As indicated below by means of ^{1}H NMR spectra and cyclic voltammograms obtained in the course of the reaction, the early part of the reduction (10−45 min) features the generation of an additional species that eventually is transformed (most likely by further reduction) to **4**. The interference of this uncharacterized intermediate is also suggested by the air sensitivity of these early solutions, which after removal of Zn rapidly afford olive-green solutions that are not due to the initial compound **2**. In contrast, pure **4** is stable to dioxygen for prolonged periods of time. The identity of the intermediate species has not been elucidated yet, but the similarity of its ^{1}H NMR spectrum (see Figure S3, Supporting Information) to that obtained for **2**, especially in regard to the close spacing of bound pyridine resonances for 3-*H* ($\delta = 7.8$) and 4-*H* ($\delta = 7.9$), suggests that the complex may feature a similar mixed-valent μ-oxo, μ-acetato core.

Table 1. Crystallographic Data[a] for $[Ru_3O(O_2CCH_3)_6(py)_3]$ (**2**)

formula	$C_{27}H_{33}N_3O_{13}Ru_3$
fw	910.77
cryst syst	rhombohedral
space group	*R*3
Z	3
a, Å	17.436(4)
b, Å	17.436(4)
c, Å	10.907(3)
α, deg	90
β, deg	90
γ, deg	120
V, Å^3	2872(1)
temp, K	213(2)
color	yellow-brown
$d_{calc,}$ g/cm^3	1.580
μ, mm^{-1}	1.226
GOF on F^2	1.337
$R1^b$ (wR2[c]), %	4.70 (13.19)

[a] Obtained with graphite monochromated Mo Kα ($\lambda = 0.710\ 73$ Å) radiation. [b] $R1 = \sum||F_o| - |F_c||/\sum|F_o|$. [c] $wR2 = \{\sum[w(F_o^2 - F_c^2)^2]/\{\sum[w(F_o^2)^2]\}^{1/2}$.

All attempts to reduce **2** by H_2/PtO_2 to gain access to a previously reported[16b] yellow species assigned to $[Ru^{II}_3(O_2CCH_3)_6(py)_3]$ have failed to provide any such species. The method provides yellow-brown solutions of **2** free of any contamination by $[\mathbf{2}]^+$, but no further reduction to any other Ru^{II} compound is observed.

Mechanistic Investigations of Gif^{IV}-Type Oxygenations. (a) Time Profile Studies of Cyclohexane Oxygenation under Gif^{IV}-Type Conditions. Given the heterogeneous nature of the Gif^{IV} reaction using stirred powdered zinc, there have been very few attempts to standardize the exact reaction conditions (among others, type of reaction vessel and stirring speed). We report herein detailed time profile studies of the appearance of products in comparative Gif^{IV}-type reactions in pyridine/acetic acid (10:1 v/v) for the first time under standardized conditions. Samples from the reaction solutions are taken at various time intervals using slight modifications to the methods previously reported by Barton and Schuchardt[27,28] (see Experimental Section). Exact comparative studies of the iron- and ruthenium-catalyzed Gif^{IV}-type reactions have been carried out for the first time. It is very clear from this work that different conditions applied to the catalytic reactions have quite a profound effect on the rates, yields, and product selectivity.

Results showing the comparative performance of the ruthenium and iron Gif^{IV}-type systems at two stirring speeds, 750

(23) Sheldrick, G. M. *SHELXS-97, Program for the Solution of Crystal Structure*; University of Göttingen: Göttingen, Germany, 1997.
(24) Sheldrick, G. M. *SHELXL-97, Program for the Refinement of Crystal Structure*; University of Göttingen: Göttingen, Germany, 1997.
(25) *SHELXTL 5.10, Program Library for Structure Solution and Molecular Graphics*, PC version; Bruker Analytical X-ray Systems: Madison, WI, 1998.
(26) Walsh, J. L.; Baumann, J. A.; Meyer, T. J. *Inorg. Chem.* **1980**, *19*, 2145.
(27) Barton, D. H. R.; Boivin, J.; Hill, C. H. *J. Chem. Soc., Perkin Trans. 1* **1986**, 1797.
(28) Schuchardt, U.; Mano, V. In *New Developments in Selective Oxidation*; Centi, G., Trifiro, F., Eds.; Elsevier: Amsterdam, 1990; p 185.

Table 2. Comparison of Gif^{IV} Oxygenating Systems

catalyst system	total oxidized product yield[a] (%)	selectivity CyO/CyOH	TN[b]
$[Fe_3O(O_2CCH_3)_6(py)_3]\cdot py$ (**1**)			
at 750 rpm	8.8	9.4	126
at 1000 rpm	9.3	8.4	133
$[Ru_3O(O_2CCH_3)_6(py)_3]$ (**2**)			87
at 750 rpm	6.1	3.1	87
at 1000 rpm	4.7	1.0	67
trans-$[Fe(O_2CCH_3)_2(py)_4]$ (**3**)[c]	16.7	6.1	239
trans-$[Ru(O_2CCH_3)_2(py)_4]$ (**4**)[c]	5.3	10.5	75

[a] Based on substrate. [b] Moles of oxidized products per mole of catalyst at the maximum yield. [c] Stirred at 1000 rpm.

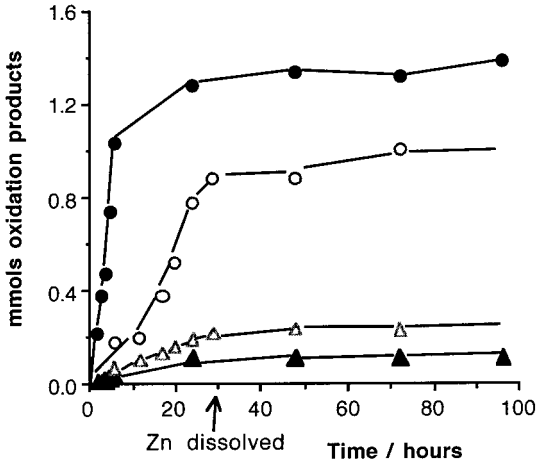

Figure 1. Time course of product formation (cyclohexanone (circles), cyclohexanol (triangles)) for both Fe and Ru−Gif^{IV} reactions stirred at 750 rpm using $[M_3O(O_2CCH_3)_6(py)_3]$ (M = Fe (filled symbols) or Ru (open symbols)) as the added metal species.

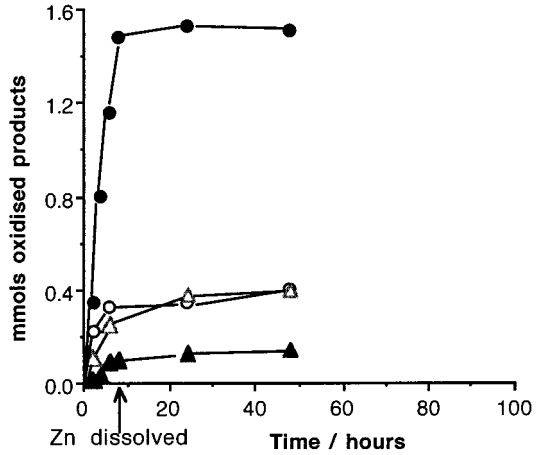

Figure 2. Time course of product formation (cyclohexanone (circles), cyclohexanol (triangles)) for both Fe and Ru−Gif^{IV} reaction mixtures stirred at 1000 rpm using $[M_3O(O_2CCH_3)_6(py)_3]$ (M = Fe (filled symbols) or Ru (open symbols)) as the added metal species.

and 1000 rpm, are shown in Table 2 and in Figures 1 and 2. The powdered zinc dissolves more rapidly as expected at the faster stirring speed, being consumed within 7−8 h at 1000 rpm as opposed to needing 29 h at 750 rpm. Clearly apparent from Figures 1 and 2, however, is that oxygenation only occurs when zinc powder is present and presumably still being consumed in the reaction solutions. The time to maximum yield of products parallels exactly the time taken for consumption of the zinc. In both the iron− and the ruthenium−Gif^{IV} reactions, for which the mixtures were stirred at 750 rpm, cyclohexanone is detected in the solution after 45 min, whereas cyclohexanol is not detected until some 6 h into the reaction. For the reactions when the mixtures are stirred at the faster speed of 1000 rpm, only 30 min is required before cyclohexanone was detected in the iron−Gif^{IV} reaction, whereas 45 min is still required before detection in the ruthenium−Gif^{IV} reaction. In both cases cyclohexanol is detectable after 2.5 h with the maximum yield of products reached in ∼10 h.

Significant differences between the two systems in terms of the -one/-ol product distribution can be seen at the different stirring speeds. For the iron system the ketone is the dominant product over alcohol for both speeds, with an increased selectivity for the ketone apparent at the slower stirring speed. However, there are significant changes to the product distribution at the two stirring speeds for the ruthenium system. When the mixture is stirred at 750 rpm, the reaction is less selective for ketone than in the iron system, but the ketone remains the dominant product. However, when the mixture is stirred at 1000 rpm, the ketone and alcohol are formed in almost comparable amounts but with a reduced overall yield compared to that observed at 750 rpm. Closer inspection reveals that for the ruthenium system this is due to a dramatic loss in the yield of ketone.

The turnover numbers (Table 2) are quite comparable for both the iron and ruthenium systems at both stirring speeds. The iron−Gif^{IV} system remains superior in both turnover and in a higher overall yield of total products (about 8−10% for iron compared to 4−7% for ruthenium). The iron system also exhibits a significantly higher selectivity for the ketone over the alcohol versus the ruthenium system (∼10:1 for iron; ∼1:1 to 3:1 for ruthenium). This observation is believed to have important mechanistic implications.

(b) ^{1}H NMR Monitoring of the Products of the Gif^{IV} Reaction. NMR monitoring was of interest in order to provide a quantitative picture of the relative amounts of the different oxygenated products seen in the various stages of the Gif^{IV} reaction not possible within the limitations of the GC−MS method. This is particularly interesting for $[Ru_3O(O_2CCH_3)_6(py)_3]$ (**2**), wherein changes to the solution composition during the early stages of the reaction (vide infra) might be correlated with the appearance of different products. Furthermore, there has been no previous attempt at monitoring the progress of a Gif^{IV} reaction by ^{1}H NMR to reveal product intermediates (for instance, *sec*-alkylhydroperoxides).

A comparative study of the iron- and ruthenium-catalyzed Gif^{IV} systems has been carried out. The use of NMR, however, necessitated reaction conditions that are much higher (10 times) in substrate than those noted above or employed under Barton's original conditions. The experimental details are described below. The iron−Gif^{IV} reaction was sampled every 30 min up to 2 h, thereafter every hour up to 5 h, and then again after 12 h (overnight). The ruthenium−Gif^{IV} reaction was sampled after 30 min, after 1, 2, and 3 h, and again after 16 h (overnight). Cyclohexane exhibits a characteristic singlet at δ 1.36 (12H) due to equivalent protons on the NMR time scale at room temperature (23 °C). The resonances used for the identification of the oxygenated products were respectively that at δ 2.25 for the ketone (t, 4H, CH_2 ortho to C=O) and that at δ 3.75−3.81 for the alcohol (m, 1H, C*H* adjacent to OH). In addition, resonances from the 0.5 H atom % of pyridine-d_5 are seen as singlets at δ 8.72 (2*H*-py), 7.62 (4*H*-py), and 7.25 (3*H*-py), respectively, and act as useful additional reference lines. The presence of water as it builds up as a product in the reaction solutions is characterized by a broad envelope observed down-

field of δ 11, which slowly drifts upfield into the pyridine region and beyond as its concentration increases. Detailed ^{1}H NMR spectra obtained for both the iron and ruthenium reactions are available as Supporting Information (Figures S1 and S2).

Notable differences in the appearance of products between the iron and ruthenium Gif^{IV} reactions are seen in the early stages (first few hours), particularly regarding the appearance of cyclohexanol. In the reactions monitored by GC−MS and in previous studies,[14,29] relatively larger amounts of cyclohexanol compared to the ketone build up in the ruthenium-based system than in the iron reaction. Under the conditions of the ^{1}H NMR experiments the alcohol appears much earlier in the ruthenium−Gif^{IV} reaction, its presence detected within 30 min of the start of the reaction before any ketone is seen. In complete contrast, the little cyclohexanol that is produced in the iron reaction does not begin to appear under the same conditions until at least 4 h into the reaction, long after the buildup of ketone. Moreover, ketone production begins in the iron reaction within 30 min, which is well before its appearance in the ruthenium reaction (1 h). These results lead one to suspect that the catalyst responsible for the production of ketone in the ruthenium system is not formed immediately but forms slowly over the first hour or so during changes observed in the composition of the solution (vide infra). For the iron reaction it appears that the active catalyst(s) form(s) quite quickly, long before the production of alcohol is seen. Mechanistic implications of these observations will be discussed.

A further weak feature that develops in the ^{1}H NMR spectra of both systems after around 3−4 h is a sharp singlet at δ 2.70 that has been identified as due to cyclohexane-1,4-dione. This same overoxidation product has also been reported in the studies carried out by Schuchardt.[28] In all the experiments conducted, there is no evidence for cyclohexylhydroperoxide as a long-lived-enough species to be detected by ^{1}H NMR in the Gif^{IV} solutions. However, it is not possible to rule out the alkylhydroperoxide as an intermediate on this basis, since further studies have demonstrated a very short half-life for this species in the presence of both divalent iron[7a] and zinc powder.[30]

(c) Investigation of the Metal Species Present during Turnover in the Gif^{IV} Reaction. (i) Iron−Gif^{IV} System. Carefully controlled chemical reductions on $[Fe_3O(O_2CCH_3)_6(py)_3]\cdot$py (**1**) with zinc have been previously carried out under Gif^{IV} conditions and the resulting compounds characterized by structural methods. A range of monomeric, dimeric, and trimeric iron and even mixed dimeric and trimeric Fe/Zn species are formed under the various conditions.[17] Crystallization directly from pyridine/acetic acid mixtures affords pale-green *trans*-$[Fe(O_2CCH_3)_2(py)_4]$ in 80% yield. However, if diethyl ether is diffused into the solution, polymeric diferrous $[Fe_2(O_2CCH_3)_4(py)_3]_n$ can be isolated in 40% yield often contaminated with *trans*-$[Fe(O_2CCH_3)_2(py)_4]$, $[Zn(O_2CCH_3)_2(py)_2]$, and a mixed iron/zinc complex $[Zn_2Fe(O_2CCH_3)_6(py)_2]$ (linear structure). Interestingly, the diferrous unit of the polymeric complex has a structure reminiscent of that present in the active site of the reduced form of soluble methane monooxygenase (sMMO).[31]

In the absence of facile ^{1}H NMR monitoring due to paramagnetism and fast exchange of ligand/solvent molecules, we have carried out studies of the changes taking place in these solutions using cyclic voltammetry on glassy carbon. Voltammograms of fresh deoxygenated solutions of $[Fe_3O(O_2CCH_3)_6(py)_3]\cdot$py (**1**) (5 mM) in pyridine/acetic acid (10:1 v/v) show a one-electron process at +0.025 V versus Ag/AgCl (Fe_3(III,III,III) → Fe_3(III,III,II)) (reversible) and a two-electron process at −0.9 V (Fe_3(III,III,II) → 3Fe(II)) (irreversible). Upon treatment with zinc powder an immediate color change from greenish-brown to pale-green is seen and the voltammogram now consists of a single reversible process at −0.05 V along with a number of irreversible features in the region more cathodic of −0.3 V. There are no features seen corresponding to the original complex $[Fe_3O(O_2CCH_3)_6(py)_3]\cdot$py (**1**). From studies of an authentic sample of *trans*-$[Fe(O_2CCH_3)_2(py)_4]$ (**3**) prepared separately, the wave at −0.05 V is due to the Fe(III)/Fe(II) process for the divalent complex **3**.

(ii) Ruthenium−Gif^{IV} System. The low-spin nature of the ruthenium species and the slow ligand/solvent exchange allows monitoring of the changing solution composition by both cyclic voltammetry and by ^{1}H NMR in solutions of pyridine-d_5/acetic acid-d_4.

Cyclic voltammograms of freshly deoxygenated solutions of $[Ru_3O(O_2CCH_3)_6(py)_3]$ (**2**) in pyridine show two reversible couples at +0.05 V versus Ag/AgCl (Ru_3(III,III,III) → Ru_3(III,III,II)) and at −1.3 V (Ru_3(III,III,II) → Ru_3(III,II,II)) (Figure 3). No change occurs upon addition of acetic acid (py/AcOH 10:1 v/v) within the available window. Upon the addition of zinc, however, nothing happens within a few minutes (the time taken for the corresponding trinuclear iron complex to disappear), but eventually a new redox couple centered at +0.45 V appears on the voltammogram within 10 min, which in turn disappears after about 45 min (Figure 3) to be replaced by two further quasi-reversible couples at +0.2 V (major) and −0.2 V (minor). The latter two features remain visible in the cyclic voltammograms of these solutions after several days. This metastable behavior is also seen for new peaks appearing at −0.4 V (oxidation) and −0.8 V (reduction). The couple at +0.2 V reaches maximum intensity after 3−5 h. From studies of an authentic sample, the couple at +0.2 V (in addition to the minor component at −0.2 V) is due to the presence of the divalent complex *trans*-$[Ru(O_2CCH_3)_2(py)_4]$ (**4**) in these solutions. From roughly 3 h into the reaction up to 1 day, a further irreversible oxidation wave grows in around +0.5 V, which eventually envelopes the anodic wave of the +0.2 V couple of **4**. This wave at +0.5 V is also seen in the iron-containing solutions and is believed to correlate with background reactions involving pyridine and zinc/O_2 because all three of these components, in addition to metal (Ru or Fe), are needed. The appearance of these new waves also accompanies a distinct browning of the solutions, a feature also seen, but occurring more slowly, in the absence of a metal complex. Under the conditions of the CV experiments the zinc is found to completely dissolve after about 1 day.

^{1}H NMR spectra were taken at 10, 55, and 165 min intervals after the addition of zinc powder to a solution of $[Ru_3O(O_2CCH_3)_6(py)_3]$ (**2**) in pyridine-d_5/acetic acid-d_4. These spectra are available as Supporting Information (Figure S3). The ^{1}H NMR spectrum of **2** before zinc addition shows a singlet for the acetate methyl groups at δ 2.26 in addition to resonances for bound pyridine at δ 8.73 (d, 2-*H*-py), 7.77 (t, 4-*H*-py), and 7.67 (t, 3-*H*-py). These resonances were easily distinguishable from those of free undeuterated solvent pyridine by shift and

(29) Powell, G. Ph.D. Thesis, University of St. Andrews, Scotland, 1991.
(30) Separate studies have shown that stirred zinc powder reacts with cyclohexylhydroperoxide in pyridine/acetic acid (10:1 v/v) to give a 70% yield of cyclohexanol within 5−10 min. Marr, S. B.; Richens, D. T. *ACH—Models Chem.* **1998**, *135*, 821.
(31) (a) Rosenzweig, A. C.; Nordlund, P.; Takahara, P. M.; Frederik, C. A.; Lippard, S. J. *J. Chem. Biol.* **1995**, *2*, 409 and references therein. (b) Rosenzweig, A. C.; Lippard, S. J. *Acc. Chem. Res.* **1994**, *27*, 229. (c) Rosenzweig, A. C.; Frederik, C. A.; Lippard, S. J.; Nordlund, P. *Nature* **1993**, *366*, 537.

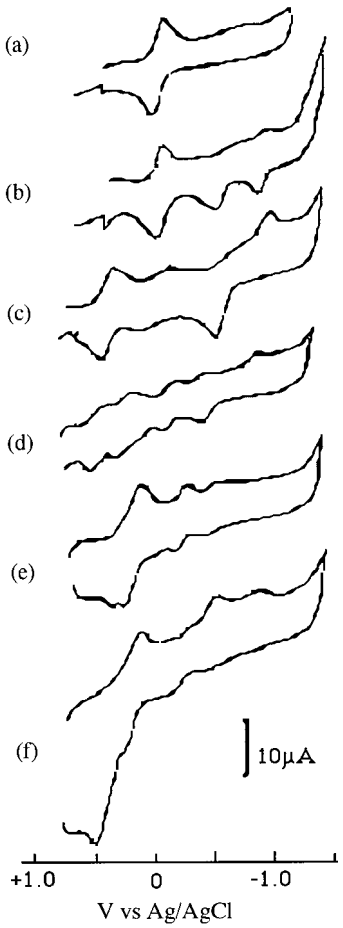

Figure 3. Cyclic voltammograms for a solution of $[Ru_3O(O_2CCH_3)_6(py)_3]$ (**2**) (5.0 mmol dm^{-3}) in pyridine (10 mL) and acetic acid (1 mL) recorded at various times following the addition of zinc powder (0.44 g) (electrolyte, 0.1 mol dm^{-3} $[Bu_4N](PF_6)$): (a) 0 min; (b) 2 min; (c) 10 min; (d) 30 min; (e) 5 h; (f) 1 day.

by the presence of proton coupling. Exchange between bound and free pyridine in this complex is slow at ambient temperature.[32,33] Upon addition of zinc, the characteristic signals for $[Ru_3O(O_2CCH_3)_6(py)_3]$ (**2**) disappear quickly to be replaced after 10 min by new singlet methyl (acetate) signals at δ 2.13 and 2.16. Over a period of several hours the δ 2.16 singlet disappears in favor of the singlet at δ 2.13 and a new singlet at δ 2.09. Separate studies reveal that the singlet at δ 2.09 is due to the free acetate ion, while the singlet at δ 2.13 corresponds to acetate protons of *trans*-$[Ru(O_2CCH_3)_2(py)_4]$ (**4**). The aliphatic/aromatic proton intensity ratio decreases over time, consistent with the slow exchange of bound acetate in the developing ruthenium products with the deuterated form in the solvent.

In the aromatic region of δ 7.0−10.0 rapid changes are seen accompanying the addition of the zinc. The pyridine signals for $[Ru_3O(O_2CCH_3)_6(py)_3]$ (**2**) are quickly lost to be replaced after 10 min (quite cleanly) by two new sets of signals for bound pyridine (evidence of coupling). The more intense signals are found at δ 9.8 (d, 2-*H*-py), 7.9 (t, 4-*H*-py), and 7.8 (t, 3-*H*-py). The less intense signals are at δ 8.9 (d, 2-*H*-py), 7.6 (t, 4-*H*-py), and 7.1 (t, 3-*H*-py). From a ^{1}H NMR spectrum taken from an authentic sample in the same solvent these latter signals are due to the pyridine protons of *trans*-$[Ru(O_2CCH_3)_2(py)_4]$ (**4**),

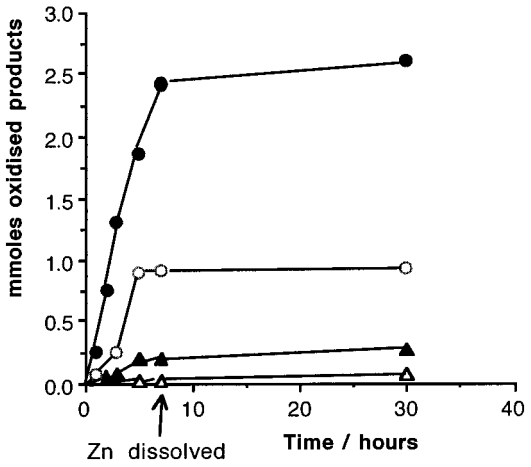

Figure 4. Time course of product formation (cyclohexanone (circles), cyclohexanol (triangles)) for both Fe and Ru−Gif^{IV} reactions stirred at 1000 rpm using *trans*-$[M(O_2CCH_3)_2(py)_4]$ (M = Fe (filled symbols) or Ru (open symbols)) as added metal species.

confirming the results from electrochemistry. It can be very easily seen in the ^{1}H NMR spectra that under these conditions the divalent monomer forms very quickly (within 10 min). The color change to orange-brown within 15 min is also consistent with formation of the divalent monomer quickly in these solutions. Over a period of 1−3 h the latter set of pyridine signals grows further in intensity at the expense of a corresponding decrease in the former signals to eventually reveal *trans*-$[Ru(O_2CCH_3)_2(py)_4]$ (**4**) as the major ruthenium-containing product in these solutions. It is therefore tempting to assign the former set of signals to the pyridine protons of the intermediate species responsible for the redox wave at +0.45 V. As noted above, this species may retain a mixed-valent μ-oxo μ-acetato-bridged structure.

(d) Studies of Gif^{IV}-Type Oxygenations of Cyclohexane Using *trans*-$[M(O_2CCH_3)_2(py)_4]$ (M = Fe, Ru) as the Added Metal Species. In view of the observation that divalent *trans*-$[M(O_2CCH_3)_2(py)_4]$ (M = Fe or Ru) complexes are the major component of the respective Gif^{IV} reaction solutions during turnover (ketone production) it was decided to carry out Gif^{IV} oxygenations on cyclohexane using these complexes as the added metal species under the same standardized conditions as used for the trinuclear precursors. These results are displayed in Table 2 and illustrated in Figure 4.

A number of features are observed. First, the total yield of oxidized products is found to increase on using the divalent complexes as catalyst precursors. However, the most significant finding is the marked selectivity toward the ketone now seen in the ruthenium system even at the faster stirring speed. This provides clear evidence of a correlation between the presence in the solutions of divalent monomer and efficient ketone production. Moreover, use of *trans*-$Fe(O_2CCH_3)_2(py)_4]$ (**3**) is found to give the highest yield of oxidized products (nearly 17% conversion based on substrate, turnover number 239 based on catalyst; Table 2) of all the metal complexes used, and the fastest rate of initial turnover (mostly ketone production) under the given conditions (Figure 4), while retaining the same overall selectivity seen when the trinuclear complex is used.

In addition, the respective times of appearance of ketone and alcohol for each systems also give clues as to the mechanistic pathways for their formation. When the trinuclear complexes are used, a significant amount of alcohol is seen early in the reaction when the ruthenium complex is employed and then the amount levels off as ketone is produced. For the iron

(32) Abe, M.; Sasaki, Y.; Yamaguchi, T.; Ito, T. *Bull. Chem. Soc. Jpn.* **1992**, *65*, 1585.
(33) Sasaki, Y.; Nagasawa, A.; Tokiwa-Yamamoto, A.; Ito, T. *Inorg. Chim. Acta* **1993**, *212*, 175.

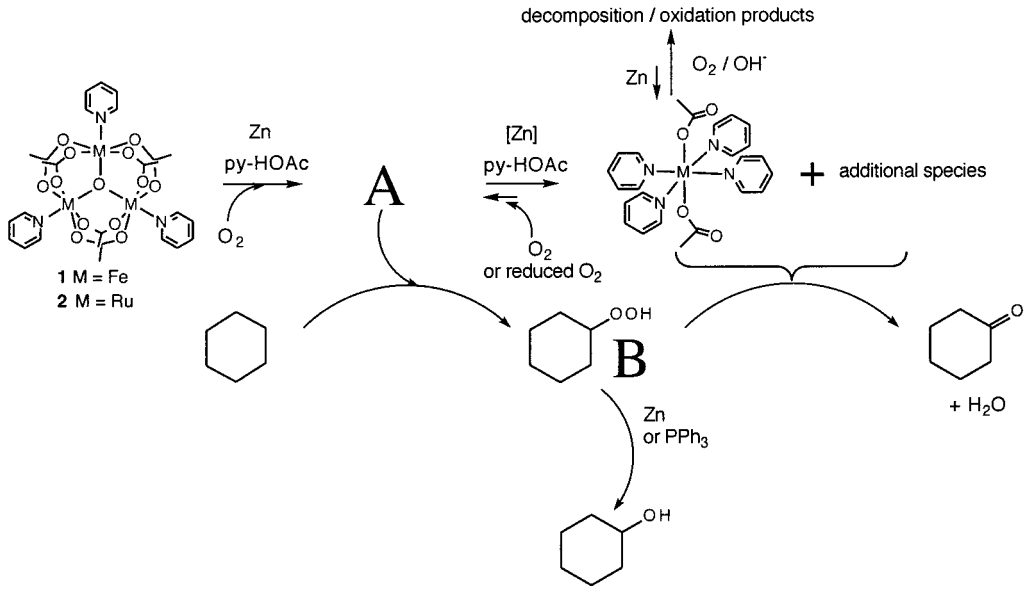

Figure 5. Reaction mechanism of the Gif^{IV} reaction. **A** and **B** are the previously defined Barton intermediates.

complex the opposite is true, since alcohol formation is only seen much later when the ketone yield has largely maximized. Thus, ketone production efficiency correlates exactly when a significant amount of the freshly generated divalent *trans*-[$M(O_2CCH_3)_2(py)_4$] complex is present. For ruthenium, ketone generation is observed to continue over a longer time period (Figure 1), as long as there is zinc in the solution to regenerate *trans*-[$Ru(O_2CCH_3)_2(py)_4$] (**4**). In contrast, alcohol formation is only observed in the later stages for the iron system when it is believed irreversible degradation of *trans*-[$Fe(O_2CCH_3)_2(py)_4$] (**3**), or its precursor, correlates with a fall-off in ketone production. In both cases the respective activity toward ketone production correlates with the steady-state concentrations of *trans*-[$M(O_2CCH_3)_2(py)_4$] in the Gif^{IV} solutions as monitored by cyclic voltammetry. Taken together, these observations point to a general scheme of reactions (see below) wherein a reduced form of the trinuclear metal complex (divalent monomer or other) reacts with O_2 (or a reduced form) to generate the active C−H activation catalyst, which eventually generates the *sec*-alkylhydroperoxide from the cycloalkane. This is a relatively fast process for both metals and points largely toward a C−H activation step that is mediated by oxygen-centered radical(s). The relative amounts of ketone and alcohol produced are then a consequence of competing reactions on the *sec*-alkylhydroperoxide, zinc reduction to give alcohol, or reaction of hydroperoxide with divalent metal (fast)[7a] or trivalent metal (slow)[30] to give ketone. When the trinuclear ruthenium complex is used, alcohol production is seen early presumably because of slow assembly of the active ketonizing catalyst (correlating with the slower buildup of *trans*-[$Ru(O_2CCH_3)_2(py)_4$] in the solutions).

The relative efficiencies of these two reactions can be tuned by the stirring speed, slow stirring favoring ketone production, whereas faster stirring gives relatively more alcohol correlating with a more vigorous reaction of the heterogeneous zinc reductant with a common intermediate, the *sec*-alkylhydroperoxide. It is conceivable that the rate of reduction is surface-dependent by providing high specific (and acid-washed) surface area with increasing stirring capacity.

Conclusions

The observations collected above suggest the following overall mechanism (Figure 5) for the Gif^{IV} reaction.

Intermediate **A** is defined as the species initially responsible for the C−H activation step to produce the alkylhydroperoxide. Barton[1] has proposed that **A** is a high-valent iron oxenoid (Fe^V=O), effectively equivalent to $Fe^{II}-O_2^-$ (Gif^{IV} system) or $Fe^{III}-OOH^-$ (GoAgg system), to explain the unusually high 2°/3° ratios observed and low kinetic isotope effect values (~2.0 for the ketone). However, strong evidence is now available via investigation of Fe^{III}/H_2O_2-dependent Gif-type systems[13] to suggest that the active oxidants are oxygen-centered radicals ($HO^•/RO^•$). The more gradual changes observed within the Ru−Gif^{IV} solutions coupled with the time of appearance of ketone have provided an insight into the various steps in the Gif^{IV} reaction. Alcohol can clearly accummulate before the divalent monomer complex *trans*-[$Ru(O_2CCH_3)_2(py)_4$] (**4**) is fully assembled. Thus, the formation of **4** is not required for alcohol production, but it is related to efficient ketone production as verified in separate studies. This can be explained in terms of the [$Ru_3O(O_2CCH_3)_6(py)_3$] (**2**) fragmenting within 15 min upon reduction with zinc to afford an early ruthenium precursor species with a different pyridine/acetate stoichiometry to *trans*-[$Ru(O_2CCH_3)_2(py)_4$] (**4**), possibly featuring a mixed-valent oligonuclear site richer in O-donor acetate ligands[17] than **4**, which reacts with O_2 (or O_2^-)[34,35] to eventually generate **A**. The immediate precursor to **A** is probably a reduced metal complex of average valency below +3. **A** then makes *sec*-alkylhydroperoxide from the alkane via C−H activation. This has to take place fairly quickly for both metals, within the first 30 min, since alcohol, arising from zinc reduction of hydroperoxide,[30] is seen already in the solutions of the Ru system after this time.

The fate of the alkylhydroperoxide is then 2-fold. Either it can react with further metal species in the solution to generate ketone, or via reducing agents in the solution (zinc powder[30] or PPh_3[7a]) to form alcohol. Since ketone appearance correlates well with the time of appearance of *trans*-[$M(O_2CCH_3)_2(py)_4$], this complex, or another related species formed in the solution at exactly the same time (as additional features are seen in the cv's of **4** in the presence of acetic acid (Figure 3)), would seem likely candidates for the active species involved in alkylhydro-

(34) Carley, A. F.; Roberts, M. W.; Tomellini, M. *J. Chem. Soc., Faraday Trans.* **1991**, *87*, 3563.
(35) Roberts, M. W. *Chem. Soc. Rev.* **1996**, *25*, 437.

peroxide decomposition and ketone production in the Gif^{IV} reaction. This is further supported by the observation (Figure 4) that when *trans*-[$Ru(O_2CCH_3)_2(py)_4$] (**4**) is used as catalyst, there is a significant lag time before the ketone starts to build up, more than in the case when [$Ru_3O(O_2CCH_3)_6(py)_3$] (**2**) is used under the same conditions (Figure 2). This lag time is not apparent when *trans*-[$Fe(O_2CCH_3)_2(py)_4$] (**3**) is used, and thus, the behavior of the Ru system may also be a consequence of slower rates of reaction (substitution) of alkylhydroperoxides at the more inert *trans*-[$Ru(O_2CCH_3)_2(py)_4$] (**4**) complex.

All of the above observations are consistent with formation of and subsequent reactions involving the *sec*-alkylhydroperoxide as the key hydrocarbon-derived intermediate in Gif^{IV} and probably all Gif-type oxygenations on cyclic ring hydrocarbons.

Acknowledgment. We thank the EPSRC (U.K.) for the award of an earmarked studentship (S.B.M.). We also thank the School of Chemistry, University of St. Andrews for provision of an M.Phil scholarship (R.O.C.). The present work was generously supported by grants from the U.S. Environmental Protection Agency (R823377-01-1 to P.S.) and the donors of the Petroleum Research Fund administered by the ACS (ACS-PRF-29383-G3 to P.S.).

Supporting Information Available: Figures S1−S3 containing relevant NMR spectra as described in the text and an X-ray crystallographic file in CIF format for the structure determination of [$Ru_3(O)(O_2CCH_3)_6(py)_3$]. This material is available free of charge via the Internet at http://pubs.acs.org.

IC0001560